DOI: 10.1002/chem.200801512

The Binding Mode of Petrosaspongiolide M to the Human Group IIA Phospholipase A_2: Exploring the Role of Covalent and Noncovalent Interactions in the Inhibition Process

Maria Chiara Monti,[a] Agostino Casapullo,*[a] Claudio N. Cavasotto,[b] Alessandra Tosco,[a] Fabrizio Dal Piaz,[a] Arturas Ziemys,[b] Luigi Margarucci,[a] and Raffaele Riccio*[a]

In memory of Luigi Gomez-Paloma

Abstract: We report an analysis of the mechanism of human group IIA secretory phospholipase A_2 (sPLA$_2$-IIA) inhibition by the natural anti-inflammatory sesterterpene petrosaspongiolide M (PM). The amphiphilic PM, a γ-hydroxybutenolide marine terpenoid, selectively reacts with the sPLA$_2$-IIA Lys67 residue, located near the enzyme–membrane interfacial binding surface, and covalently modifies the enzyme through imine formation. Furthermore, PM is able to target the active site of sPLA$_2$-IIA through several van der Waals/electrostatic complementarities. The two events cannot co-occur on a single PLA_2 molecule, so they may contribute separately to enzyme inhibiton. A more intriguing hypothesis suggests a double interaction of PM with two enzyme molecules, one of them covalently modified and the other contacting the inhibitor through its active site. We have explored the occurrence of this unusual binding mode leading to PM-induced PLA_2 supramolecular complexes. These insights could suggest new PLA_2-inhibition-based therapeutic strategies.

Keywords: enzymes · inhibitors · natural products · phospholipases · protein interactions

Introduction

Lipids have been described as the "most overlooked molecules in biology".[1] Nevertheless, in the last few years, the long-lasting oversight of the unique biological relevance of lipids has been changing, as a consequence of feverish studies in areas like membrane biophysics, protein–lipid interactions, and cannabinoid systems, to name just a few. One of the most relevant topics, within the physiopathological implications of lipid–protein recognition, interaction, and catalysis, is undoubtedly the role of phospholipase enzymes. Phospholipases A_2 (PLA_2s) are involved in the hydrolysis of the *sn*-2 ester bond of the membrane phosphoglycerides in a regio- and stereospecific manner.[2] These enzymes are involved in several biological functions, such as membrane homeostasis, digestion, and production of precursors for lipid hormones.[3] PLA_2s are classified in 13 groups and several subgroups on the basis of their structure, molecular weight, substrate specificity, and cellular localization. Mammalian tissues contain both the Ca^{2+}-dependent secretory (sPLA$_2$s, groups I, IIA, IIC, V, and X) and cytosolic (cPLA$_2$s, group IV) enzymes, as well as some intracellular isoforms (iPLA$_2$s, group VIA).[4] sPLA$_2$s belong to a family of small (14–16 kDa), disulphide-rich, calcium-dependent enzymes, which includes human type IIA secretory PLA_2 (sPLA$_2$-IIA).[5] The latter is inactive on isolated phospholipid substrates but undergoes "interfacial activation" after correct arrangement on the phospholipid layers. The best sPLA$_2$-IIA substrates are supramolecular structures such as lipid monolayers, micelles, vesicles, and membranes; in particular, negatively

[a] Dr. M. C. Monti, Prof. A. Casapullo, Dr. A. Tosco, Dr. F. Dal Piaz, Dr. L. Margarucci, Prof. R. Riccio
Dipartimento di Scienze Farmaceutiche
Università di Salerno
Via Ponte Don Melillo, 84084 Fisciano (Italy)
Fax: (+39) 089-962-828
E-mail: casapullo@unisa.it
riccio@unisa.it

[b] Prof. C. N. Cavasotto, Dr. A. Ziemys
School of Health Information Sciences
University of Texas Health Science Center at Houston
7000 Fannin St. 860B, Houston, TX 77030 (USA)

Supporting information for this article is available on the WWW under http://dx.doi.org/10.1002/chem.200801512.

charged species are cleaved several orders of magnitude faster than zwitterionic ones.[5] The $sPLA_2$-IIA region that interacts with the outer membranes is called the interfacial binding surface (IBS) and contains six hydrophobic (Val3, Ala18, Leu19, Phe23, Phe63, and Tyr111) and two basic (Arg7 and Lys10) amino acid residues. Additionally, Lys67 and Lys107, which are located at a distance of 4–5 Å from the membrane surface, are involved in the IBS stability.[6] The starting point for this work can be found in our ongoing extensive investigation of the PLA_2-inactivation mechanism by anti-inflammatory marine natural products.[7] Among the γ-hydroxybutenolide-containing natural products, petrosaspongiolide M (PM, **1**; Scheme 1)[8] is endowed with a remarkable pharmacological profile.[9] Enticed by the prospect of the rational design of simplified inhibitors as new potential lead compounds against inflammation-related diseases,[10] we have investigated the molecular mechanism of $sPLA_2$-IIA inhibition by PM and its congener 25-*O*-acetyl-PM (PMAc, **2**; Scheme 1). The latest findings of an oncogenic action of PLA_2 in prostate cancer[11] offered further motivation for the study. Herein, we have evaluated the role of the covalent and noncovalent interactions in this inhibition process, and our results suggest that the inhibition mechanism is ruled by the two binding modes. A separate contribution of the two events or their co-occurrence in the enzyme inactivation has been investigated in detail and discussed. In the most intriguing hypothesis, PM covalently modifies one PLA_2 molecule and also (noncovalently) contacts the active site of another unit; these interactions ultimately modulate the protein–protein and protein–lipid binding.

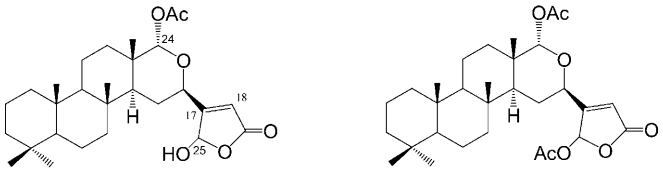

Scheme 1. Chemical structures and molecular weights (MW) of petrosaspongiolide M (PM, **1**) and 25-*O*-acetyl-PM (PMAc, **2**).

Results and Discussion

Our study of the mechanism of $sPLA_2$-IIA inactivation by PM at the molecular level consisted of the following phases: a) kinetic analysis of the $sPLA_2$-IIA inhibition profile; b) structural analysis of the protein–inhibitor complex; c) in silico generation of a 3D model of the protein–inhibitor complex by using the experimental evidence as constraints.

Kinetic analysis of $sPLA_2$-IIA inhibition: The inhibition of phospholipase activity by petrosaspongiolides was tested in an assay buffer containing dioleylphosphatidylglycerol (DOPG) vesicles with a continuous fluorescence-displacement assay.[12–14] The enzyme-inactivation rates progressively increased with the concentration of the inhibitors and reached maxima of 95 and 70% inhibition for PM and PMAc, respectively (Figure 1A). The different kinetic profiles of PM and PMAc confirmed the important role of the free hemiacetal function on the γ-hydroxybutenolide ring, as already reported for PM in a different enzymatic system;[7c] hence, the decreased effectiveness of PLA_2 inhibition by PMAc was due to the acetylation at the C25 position. Furthermore, the kinetic responses were levelled after long incubation times, and the inhibition potency of PMAc and PM became similar (Figure 1B).[7c]

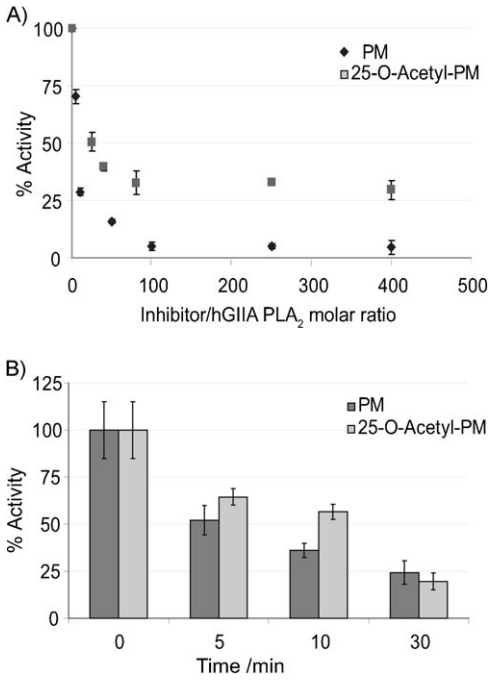

Figure 1. PLA_2 activity in the presence of PM and PMAc. A) The inhibition profile at different ligand/protein molar ratios after 10 min of incubation. B) The percentage of $sPLA_2$-IIA activity with a ten-fold molar excess of ligand after 5, 10, and 30 min of incubation. Data are the mean values ± SD of at least three different assays and are shown as a percentage. (The activity value without inhibitor was set to 100%.)

Structural analysis of PLA_2–inhibitor complexes: As in our previous studies, in which the bee venom PLA_2 was affected by both covalent and noncovalent interactions when incubated with several natural inhibitors,[7] we used a mass spectrometry approach in the analysis of the $sPLA_2$-IIA–inhibitor complexes.

To clearly characterize the PM-inactivation mode, whether competitive or not, we resorted to a selective histidine-acylating agent, *para*-nitrophenacylbromide (pNBr, molecular weight (MW) of 244 Da). This agent is well known to selectively bind the catalytic His residue of several PLA_2s, and this modification is easily revealed by MS with a measured

MW increase of 164 Da.[7e] Comparative experiments in which PLA_2 is incubated with pNBr in the presence or absence of the inhibitor hence provide valuable clues on the type of inhibition mechanism (whether competitive or not). Therefore, we incubated $sPLA_2$-IIA with pNBr and recovered, by LC–nanoESIMS, a main fraction containing $sPLA_2$-IIA modified at His47 (data not shown, see Table S1 in the Supporting Information). The same procedure was repeated with the enzyme preincubated with PM (sPLA2-IIA:PM molar ratio of 1:5) before addition of pNBr. LC–MS data revealed that $sPLA_2$-IIA was not modified by pNBr in this case, which proves the occurrence of early binding of PM to the active site of the enzyme.

Therefore, we moved on to the details of this protein–ligand interaction by incubating $sPLA_2$-IIA with PM and analyzing the reaction mixture by LC–nanoESIMS (see the Supporting Information). The chromatographic trace consisted of two peaks, which were identified by mass spectrometry as the unreacted $sPLA_2$-IIA ((13860.62 ± 0.10) Da) and its covalent 1:1 complex with PM. The latter species consisted of two multicharged ion envelopes, deconvoluted at MWs of (14320.68 ± 0.16) and (14302.24 ± 0.45) Da (see Figure S2 and Table S1 in the Supporting Information), which correspond to mass increments of 460 and 442 Da, respectively. These results were suggestive of the addition of a nitrogen nucleophilic residue on the enzyme to the C25 masked aldehyde of PM; this generates an initial hemiaminal intermediate (ΔMW = 460 Da) that evolves into a Schiff base (ΔMW = 442 Da) through loss of H_2O (Scheme 2A). The existence of an imine moiety in the $sPLA_2$-IIA–PM covalent complex was also confirmed by selective reduction with sodium borohydride ($NaBH_4$), as monitored by LC–MS (ΔMW = 444 Da). Furthermore, the PM–PLA_2 imine adduct reverted in a reaction with hydroxylamine (NH_2OH) to give rise to the PM–oxyme and the free protein.

On these grounds, we ruled out other plausible reaction pathways for the hydroxybutenolide moiety, namely Michael addition of a PLA_2 lysine residue at the C17 position (ΔMW = 462 Da) or transesterification at the C24 position (ΔMW = 442 Da, no reaction with NH_2OH). The same protocol was then applied to the case of PMAc, with identical results in terms of the mass increments. As suggested from the inhibition kinetics, MS data confirmed that, upon exposure to PLA_2, PMAc is transformed into PM by means of a nonspecific esterase activity of PLA_2 (see Scheme 2B and Table S1 in the Supporting Information). This, in turn, requires that PMAc (and hence PM) targets the inner surface of the PLA_2 active site. We then moved to the identification of the covalent-binding site on the enzyme. This part of the work was a complex task, due to the difficulties in the detection of $sPLA_2$-IIA–PM complexes in the incubation mixture. Actually, addition of PM to the PLA_2 solution induced aggregation of the complex, which complicated its recovery and recognition. This was confirmed by addition of nondenaturing surfactants, in particular, β-octyl-D-glucopyranoside (OGP), that slightly improved the complex solubility. On the basis of this behavior, we decided to carry out our analysis by sodium dodecylsulfate polyacrylamide gel electrophoresis (SDS-PAGE), in situ tryptic digestion, and MALDI-TOF mass spectrometry.[15] PLA_2 was incubated with the inhibitors (PM and PMAc) and, after reduction with $NaBH_4$, the sample was chromatographed by SDS-PAGE to eliminate the excess of inhibitor and $NaBH_4$. The same procedure was performed on the protein as a reference experiment. MALDI-TOF analysis of in situ tryptic digestion of the SDS-PAGE spots allowed us to map the entire protein sequence. A signal at m/z 1835.94 was detected only in the spectrum of the PM–PLA_2 tryptic mix (see Figure S3 and Table S2 in the Supporting Information) and was attributed to the mass of peptide fragment 63–74 with addition of 444 Da (theoretical MW of 1834.7 Da). The Lys67 residue is

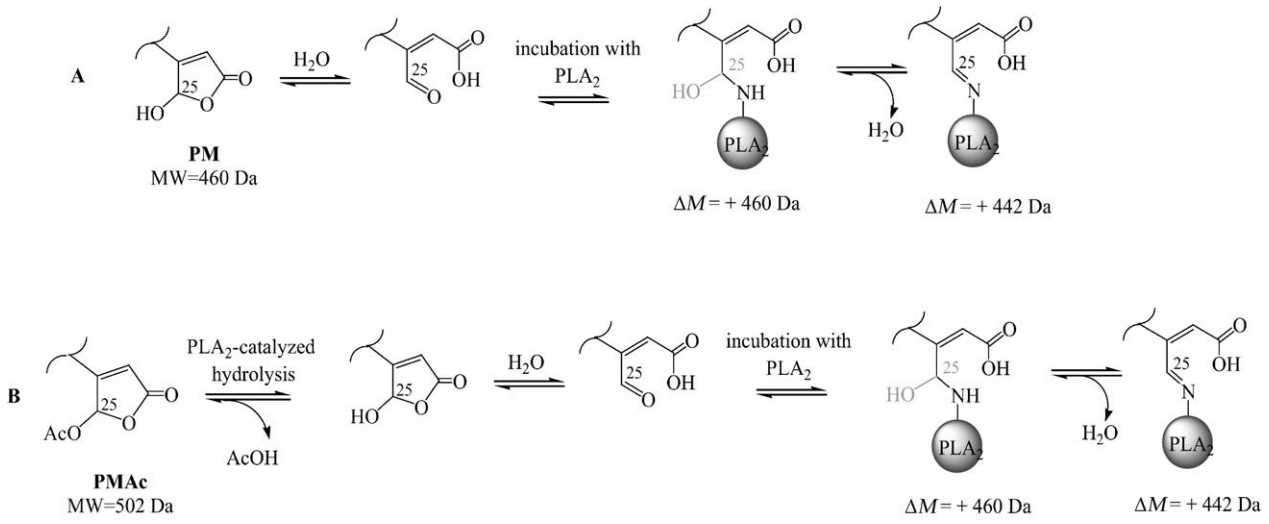

Scheme 2. Reaction mechanisms for the covalent inactivation of $sPLA_2$-IIA by A) PM and B) PMAc. Mass increments were measured by LC–nanoESIMS and account for the losses of H_2O (in A) and AcOH+H_2O (in B).

the only reactive center in the peptide 63–74 (FLSYKFSNSGSR) that is able to produce an imine by nucleophilic addition to PM. When analyzed under an identical experimental procedure, PMAc showed the same behavior as PM, which thus confirms the mechanistic hypothesis previously discussed (Scheme 2B). Therefore, the PLA_2-inhibition process seems to be ruled either by a competitive insertion of the inhibitor inside the enzyme active site driven by noncovalent forces or by the covalent modification of Lys67. This residue is closely connected to the enzyme IBS[6] and its modification can thus modulate the lipid–PLA_2 surface-recognition process during the interfacial catalysis step. On the other hand, a full picture of the inhibition process that takes into account the co-occurrence of both events on a single PLA_2 molecule is a complex task, because Lys67 is located far away from the active site. Hence, the two events could separately contribute to the enzyme inactivation, by virtue of the PM covalent modification (Lys67) of some PLA_2 molecules and the additional (noncovalent) association with the active site of other PLA_2 units.

Another intriguing hypothesis suggests a double interaction of PM with two PLA_2 molecules, one of them covalently modified at Lys67 and the other contacting the inhibitor, through noncovalent interactions, inside the active site. A fundamental observation in this context is the fact that the nucleophilic attack of Lys67 liberates a free carboxyl group in PM and, thus, generates a substrate analogue consisting of a polar negatively charged head (the COO^- group) and a large hydrophobic tail (the tetracyclic core), which is in close analogy with the structure of a phospholipid. Therefore, the Lys67-bound PM may be capable of targeting the active site of another $sPLA_2$-IIA molecule due to van der Waals/electrostatic complementarity and, importantly, through its ability to chelate the essential calcium ion with its carbonyl oxygen functionalities. In this scenario, PM would act to induce the construction of oligo- and/or polymeric supramolecular complexes. Although this appealing hypothesis is in remarkable agreement with some experimental evidence, we decided to further address its significance by means of a thorough exploration of the complementarity between the Lys67-bound PM and the active site of another PLA_2 unit by using surface plasmon resonance biosensor analysis[16] and computational techniques.

Surface plasmon resonance analysis: Initially, we measured the binding of PM with $sPLA_2$-IIA after enzyme immobilization on the sensor chip. We registered sensorgrams with a dissociation curve of about 500 s; this was followed by a plateau. The response units (RU) of the sensorgrams did not decrease to the baseline value, as a consequence of the covalent modification of the enzyme on the target (Figure 2A). This peculiar behavior was functional in the second experimental setup. In this case, a sample of freshly solubilized $sPLA_2$-IIA was injected either on to the chip surface containing $sPLA_2$-IIA covalently bound to PM or, as a reference experiment, on to the chip surface linked to the $sPLA_2$-IIA alone. The registered sensorgram (Figure 2B, gray trace), in contrast to the reference experiment (Figure 2B, black trace), displayed a typical binding profile (association and dissociation steps), which is suggestive of a PLA_2–PM–PLA_2 complex on the target (with a calculated dissociation constant (K_D) value in the μM range). This evidence supports the hypothesis of a PM-induced protein–protein interaction.

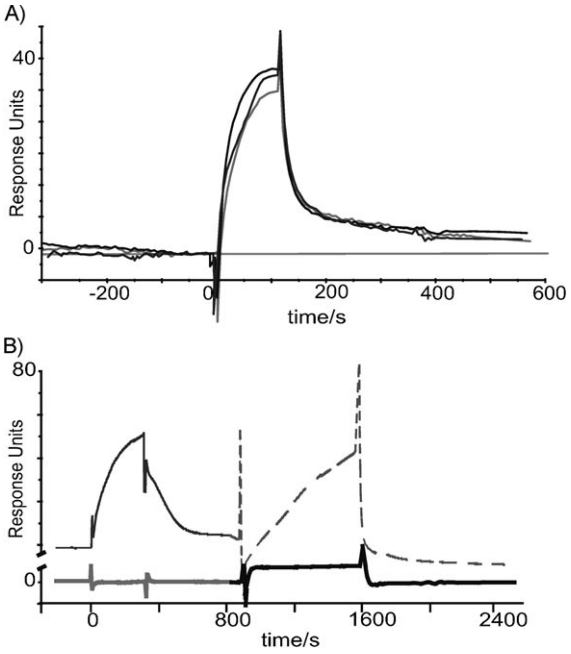

Figure 2. A) The irreversible binding of PM at 3 different concentrations (50, 100, and 200 μM) to $sPLA_2$-IIA immobilized on the sensor chip. B) The consecutive injection of PM (50 μM, solid line) and solubilized $sPLA_2$-IIA (50 nM, dashed line) on a sensor chip with immobilized $sPLA_2$-IIA. The gray and black bold solid lines were measured for the consecutive injection of buffer and solubilized $sPLA_2$-IIA (50 nM) on a sensor chip with immobilized $sPLA_2$-IIA. All sensograms were subtracted from a control-experiment trace. A colour version of this figure is available as Supporting Information.

Computational studies on PLA_2–PM–PLA_2 complex: As a final step, we resorted to a computational approach by building a plausible 3D model in support of our hypothesis. The first step was the full flexible docking into the PLA_2 pocket of a simple model compound consisting of a PM–Lys imine (PM-K). The goal of this ligand docking stage was to explore the conformational space of PM-K within the PLA_2 binding pocket and then to use these poses to align the PM portion of the real PLA_2–PM covalent adduct (PM–Lys67–PLA_2) in the protein–protein docking stage. The flexible-ligand/flexible-side-chain algorithm used has been already documented.[17–21] The PLA_2–PM–PLA_2 adduct was then built by attaching a PM molecule to Lys67. The PLA_2–PM adduct was considered as the "ligand" (in the sense that its six positional coordinates were considered to be free), and the second PLA_2 molecule was regarded as the "receptor" (whose six positional coordinates were fixed). The protein–protein docking stage began with the construction of 128 initial complexes (generated to maximize ligand-orientation di-

versity). The ensemble was further reduced through successive steps of local energy minimization to 17 nonredundant complexes. A stochastic global energy optimization was then performed on each of the 17 complexes, with the 6 positional coordinates of the ligand, the side chains at the interface, the torsional variables of PM+Lys67, and the Ca^{2+} atom being set free during the energy minimization. The best energy conformations within an energy window of 30 kcal mol^{-1} are displayed in Figure 3. It is interesting to

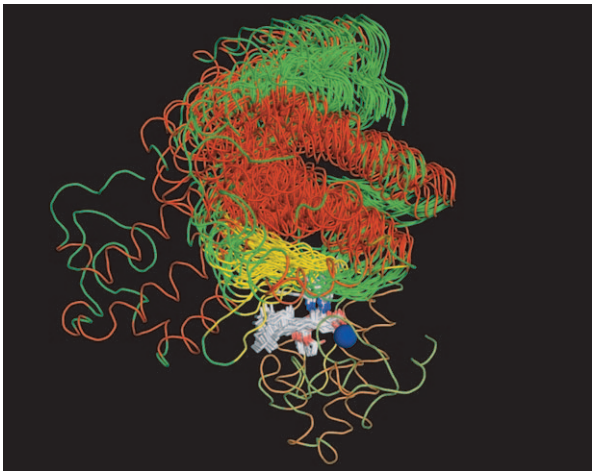

Figure 3. Ribbon representation of the lowest energy PLA_2–PM–PLA_2 complexes. All of the low-energy conformations exhibit the same binding trend. Color code: PLA_2 receptor: yellow-orange; Ca^{2+}: blue; PLA_2-PM covalent adduct: helices: red; β-sheets: yellow; loops: green. PM attached to K67 in the PLA_2-PM covalent adduct is depicted in stick representation. The picture was prepared by using the PyMol software (www.pymol.org).

note that all but one of the low-energy conformations exhibit the same binding trend. In order to study the stability, dynamic properties, and key contacts between the interacting partners, the lowest energy PLA_2–PM–PLA_2 complex was selected as a subject for molecular dynamics (MD) simulations. The initial complex was minimized, annealed (see the Supporting Information for a description of the methodology), and then subjected to MD simulation (10 ns) in a fully solvated environment. We observed that, throughout the 10 ns simulation, the complex remains compact and the structure does not significantly deviate from the starting model. Indeed, the distance between the mass centers of the two PLA_2 units was constant at around 31 Å, and the mass-weighted radius of gyration (R_g) and the root mean square deviation (RMSD), calculated in the last 5 ns of the MD simulation, were highly stable over all of the simulation steps (see Figure S4 in the Supporting Information).

The observed stability of the complex was related to the PM arrangement, because both the covalent bond with Lys67 on the first PLA_2 molecule and the chelating link to the Ca^{2+} ion on the second protein unit created rigid anchors. In fact, the PM and Asp48 carboxyl groups and the Gly31 and His27 carbonyl oxygen atoms, together with 2 water molecules, firmly coordinate the Ca^{2+} ion within a distance close to 2.5 Å (Figure 4 A and B). Moreover, one portion of the PM tetracyclic core contacts a cluster of PLA_2 hydrophobic groups, namely the Phe5, Leu2, Ile9, Ala18, Leu19, and Val30 side chains, and the Gly22 backbone atoms, whereas the rest sticks out from the pocket and turns towards the solvent (Figure 4 A).

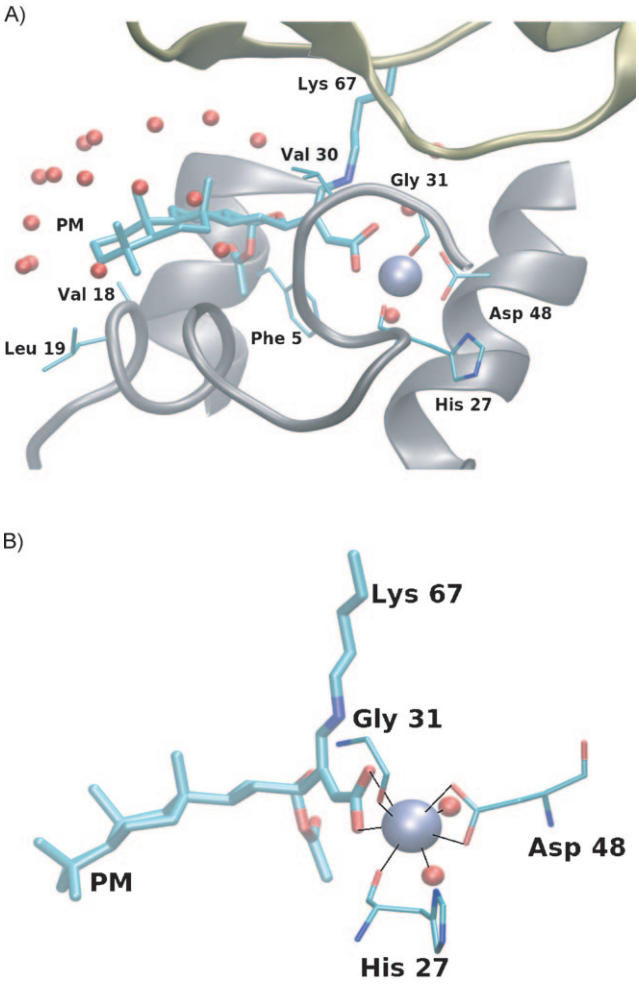

Figure 4. A) Representative PM binding-pocket structure after 10 ns of MD simulation. The PM structure is shown partly submerged into the PLA_2 (A chain: gray) protein and with chelating bonding to the Ca^{2+} ion. Water molecules (oxygen atoms: red spheres) are found mainly around the hydrophobic steroid moiety of PM. B) Close-up view of the Ca^{2+} coordination within the catalytic site. Note that Lys67 belongs to the PLA_2 unit covalently bound to PM, whereas the other residues belong to the second PLA_2 unit. See Supporting Information for further details.

The 3D model depicted in Figure 4 offers a structural illustration of the PM-induced PLA_2 supramolecular complex that accounts for the previously discussed dual-inhibition hypothesis.

Conclusion

The investigation of the binding mode of PM with human $sPLA_2$ has shown that the enzyme inhibition is ruled by both covalent and noncovalent interactions. Although, at the moment, the possibility that the two events separately contribute to the inactivation process has to be taken into account, we believe, on the basis of the reported evidence, that a dual binding mode can also take place. In this intriguing hypothesis, PM acts as a sort of cross-linking agent connecting two PLA_2 molecules (Figure 5). PM, in presence of phospholipid micelles, inserts its amphiphilic core into the lipid layer, in a manner resembling that of cholesterol.[22]- After covalent binding to the Lys67 residue on the first PLA_2 molecule, the PM lipophilic core is extracted from the lipid vesicles and targets the active site of a second PLA_2 unit through noncovalent contacts; this eventually leads to a protein–protein trans-inactivation. This peculiar dual binding mode of PM could induce an oligo- and/or polymerization process that leads to the assembly of supramolecular entities with low solubility. This unusual mechanism may provide the basis for further investigations that could be helpful in the development of new PLA_2-targeted therapeutic strategies.

Experimental Section

Phospholipase A_2 kinetic assay: $sPLA_2$-IIA activity assays were carried out by using the fluorescent probe ADIFAB, which consists of an acrylodan derivative of rat intestinal fatty acid binding protein that exhibits a shift in fluorescence upon binding to long-chain native fatty acids.[23] In each assay, the ratio (R) of 490 to 440 nm fluorescence was measured with an LS55 luminescence spectrophotometer (Perkin–Elmer) with excitation at 386 nm, excitation slits at 4 nm, and an emission slit at 8 nm. Calibration of fluorescence displacement was performed by using oleic acid as a standard. All assays were carried out at 37 °C, each measurement was repeated three times, and the reported values are means ± the standard deviation (SD). To obtain the phospholipid substrate at concentration of 60 μM in the form of small unilamellar vesicles, a stock solution of DOPG (10 mg mL^{-1} in methanol) was diluted in the assay buffer (10 mM 2-[4-(2-hydroxyethyl)-1-piperazinyl]ethanesulfonic acid (Hepes), 150 mM NaCl, 5 mM KCl, 1 mM $NaHPO_4$, 1 mM glucose, 1 mM $MgCl_2$, and 1 mM $CaCl_2$ at pH 7.4) by rapid injection.[24] Anionic vesicles of DOPG were chosen as a substrate for their high affinity with interfacial binding of $sPLA_2$-IIA. This was the first time, to our knowledge, that ADIFAB was used in a fluorescence-displacement assay with $sPLA_2$-IIA and DOPG as the substrate, so it was necessary to set up the right conditions for subsequent assays of inhibition. Aliquots of the assay buffer containing the DOPG substrate at various concentrations (0.01–10 μM) and 20 nM ADIFAB were placed in the cuvette, and the R value of the solution was registered for 1 min. $sPLA_2$-IIA (final concentration of 50 nM) was then added and the enzyme activity was monitored for 3000 s with

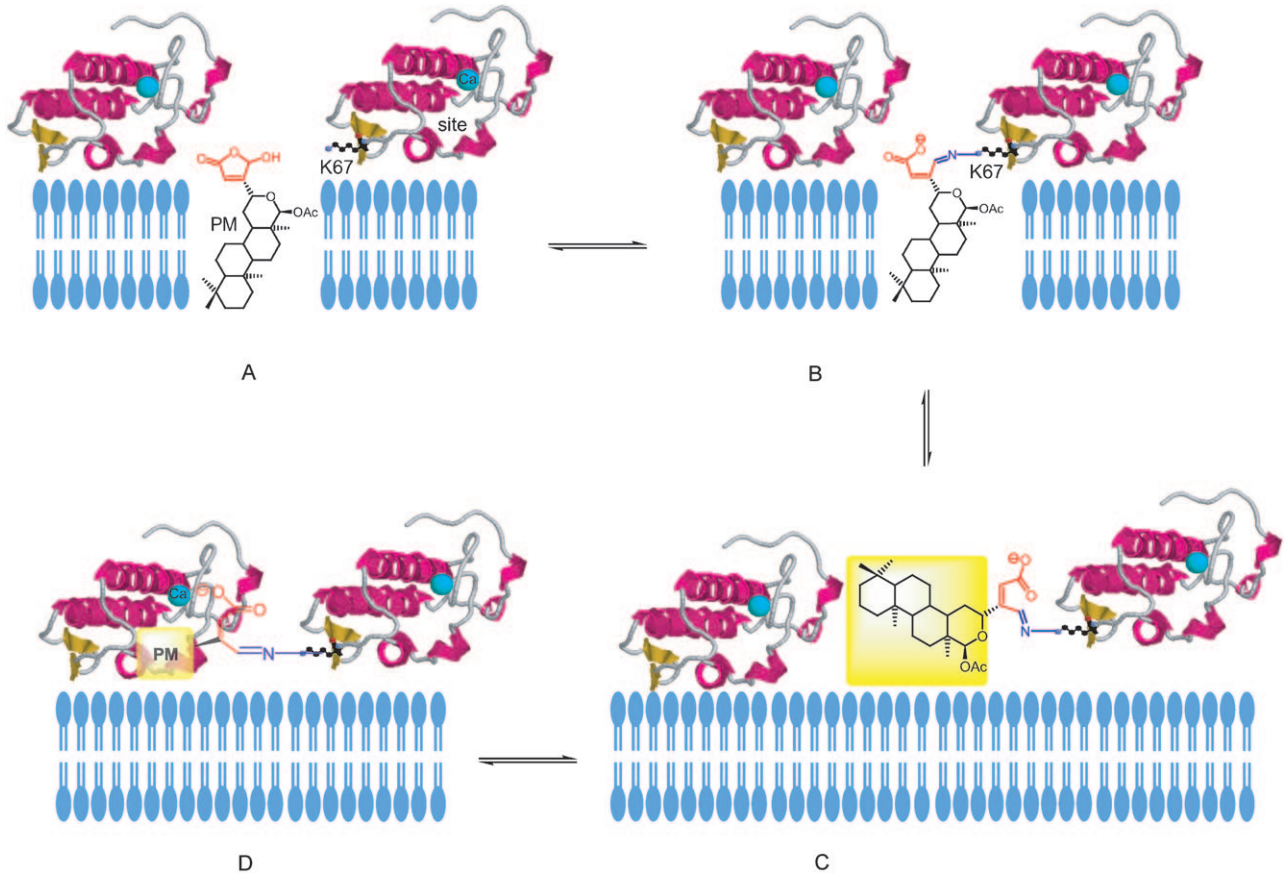

Figure 5. The supposed trans-inactivation mechanism at work: A) PM, inserted in a phospholipid bilayer, exposes its polar head towards the outer face of the membrane. B) This assists nucleophilic attack of Lys67 onto the γ-hydroxybutenolide ring and leads to an imine intermediate. C) The so-formed PLA_2-bound phospholipid-like species is released from the membrane. D) This species, acting as a substrate analogue, specifically targets the active site of another PLA_2 molecule.

an integration time of 2.0 s. A DOPG concentration of 5 μM was chosen as the saturating substrate concentration.

Kinetic analysis of inhibition: Assay buffer containing the substrate, ADIFAB, and ethylenediaminetetraacetate (EDTA; 10 mM) was placed in a fluorescence cuvette, and sPLA$_2$-IIA (final concentration of 50 nM) was added, together with different quantities of PM (final concentrations from 50 nM to 5 μM) or PMAc (final concentrations from 50 nM to 25 μM). The mixtures were incubated for 10 min at 37°C prior to addition of $CaCl_2$ (final concentration of 100 mM), and the enzyme activity was monitored. The absence of calcium as a cofactor prevented sPLA$_2$-IIA from hydrolyzing the substrate during the incubation time. In a second experimental setup, the kinetics of inhibition was monitored after 5, 10, and 30 min of incubation of the enzyme, both in presence of PM and PMAc (final concentration of 500 nM). The enzyme rate in the presence of inhibitors was then compared with that measured for the enzyme alone.

sPLA$_2$-IIA–inhibitor adduct analysis by mass spectrometry: pNBr (MW = 244 Da) was incubated with sPLA$_2$-IIA (pNBr:sPLA$_2$-IIA molar ratio of 150:1) for 5 min in phosphate-buffered saline (PBS) at a neutral pH value. The mixture was loaded on an Atlantis dC_{18} nanoAcquity column (100 mm × 75 μm) with a 5 μm Symmetry C_{18} precolumn (180 μm × 20 mm) and eluted by means of a linear gradient from 15 to 65% aqueous acetonitrile containing 0.05% trifluoroacetic acid (TFA) and 1% formic acid over a period of 25 min. Mass spectra were collected in an m/z range of 1500–3000 on an MALDI Q-ToF Premier spectrometer (Waters Co.) equipped with a nanoAcquity Ultraperformance LC system and a nanospray source. The His-specific reaction site was identified by means of a typical protocol involving disulfide reduction, cysteine alkylation, and LysC digestion followed by MALDI MS performed on a MALDI-Voyager spectrometer (Applied Biosystems). PM was dissolved in isopropyl alcohol (5 mg mL^{-1}) and added to a solution of sPLA$_2$-IIA (2 μM in 50 mM tris(hydroxymethyl)aminomethane–HCl with 10 mM $CaCl_2$ at pH 7.5) for 5 min at 25°C in fivefold molar excess. The final concentration of isopropyl alcohol in the reaction mixture was lower than 3% (v/v). The sample was alternatively treated with pNBr (as reported above) or with NH_2OH (molar ratio of NH_2OH/sPLA$_2$-IIA = 400:1) for 1 h at 37°C, or it was diluted with an equal volume of $NaBH_4$ (molar ratio of $NaBH_4$/sPLA$_2$-IIA = 400:1) in NaOH (15 mM) for 30 min at 0°C and the reaction was quenched by adding 6 M HCl (1 μL). The mixture of unreacted and modified protein was analyzed by nanoLC–MS analysis as reported above.

Location of the binding site: After incubation with PM or PMAc and reduction with $NaBH_4$, the mixture of unreacted and modified protein was centrifuged at 20800 g for 20 min. The same incubation was also performed in the presence of DOPG vesicles at the same concentration as that used in kinetic assays. The supernatant and the pellet were loaded on to a denaturing 15% SDS-PAGE gel, according to the method of Laemmli.[25] Protein bands were excised from 2–3 replicate gels. The procedure for in-gel digestion originally developed by Shevchenko et al.[26] was used with some modifications. Briefly, Coomassie-stained bands were destained and washed with 100 mM ammonium bicarbonate and acetonitrile, reduced with 1,4-dithiothreitol at 56°C for 45 min, and then alkylated with iodoacetamide in the dark for 30 min. The gel bands were incubated in a 12 ng μL^{-1} solution (50 μL) of trypsin in 50 mM ammonium bicarbonate (pH 8.0) and incubated at 4°C for 1 h. The supernatant was then removed and fresh buffer was added to cover the gel pieces during the enzymatic cleavage at 37°C overnight. The resulting peptides were extracted first with a 1:1 solution of 25 mM ammonium bicarbonate and acetonitrile and then with a 1:1 solution of 5% formic acid and acetonitrile. The extracted tryptic peptides were lyophilized and suspended with 5% formic acid (10 μL) for MALDI MS (MALDI-micro MX, Waters Co).

Surface plasmon resonance analysis: Interaction analyses were performed by using a Biacore 2000 apparatus equipped with a research-grade CM5 sensor chip (Biacore AP, Uppsala, Sweden). Amine-coupling reagents (3-(3-dimethylaminopropyl)-1-ethylcarbodiimide (EDC), *N*-hydroxysuccinimide (NHS), and ethanolamine HCl) were purchased from Biacore AB and used as described in the Biacore User Manual to immobilize sPLA$_2$-IIA in 1X PBS (pH 7.4) at a concentration of 30 μg mL^{-1}. 3 different densities of enzyme surface were prepared by using standard amine-coupling chemistry at flow rate of 5 μL min^{-1}. 7 different concentrations of PM were prepared from 10 to 300 μM, diluted in 1X PBS with 3% isopropanol, and each was injected in triplicate at flow rate of 7 μL min^{-1} by using the KINJECT command. Binding response cycles obtained for PM from the triplicate injections were superimposable, which indicated that the biosensor detection method was highly reproducible. The dissociation of the enzyme/small molecule was monitored for 5 min, and the sensor chip was efficiently regenerated between sample injections by an NH_2OH injection cycle. Data collected on the SPR biosensor were processed by the BiaEvaluation Program from Biacore AP. K_D values were calculated by using the Langmuir binding model. An sPLA$_2$-IIA solubilized sample (50 nM) was prepared in 1X PBS with 150 mM NaCl and injected on the biosensor chip modified by sPLA$_2$-IIA prior to and after injection of PM at 200 μM.

Computational methodology: Complex preparation: The crystal structure of human PLA_2 at 2.0 Å resolution (Protein Data Bank code: 1KVO) was used.[27] A water molecule close to the N terminus and the Ca^{2+} atom were also included in the receptor PLA_2 but were omitted in the ligand PLA_2 because they are far from the protein–protein interface. Based on the rigidity observed in comparing several human PLA_2 structures (unbound and bound to different ligands), the backbone structure was kept rigid during the simulations. The CC=CCOOH double bond of PM-K was kept in the *trans* configuration, as in the PM structure before the reaction with PLA_2.

Energy calculation and optimization: The molecular system was described in terms of internal coordinates, according to the Internal Coordinates Mechanics (ICM) method[28] (ICM Version 3.5-1h). The main vacuum energy terms and force-field parameters were taken from the ECEPP/3 force field,[29] by using an internal distance-dependent dielectric constant, $\varepsilon_{int} = 2 \times r$. The solvation energy contribution was based on atomic solvation parameters taken from reference [30]. For the energy reevaluation of the PLA_2–PM–PLA_2 complexes, a more accurate electrostatic energy term was calculated by solving the Poisson equation with the boundary-element algorithm (in the latter case, $\varepsilon_{int} = 2$),[31] while the nonpolar contribution to the solvation energy was assumed to be proportional to the solvent-accessible surface area (surface-tension parameter, $\gamma = 12$ cal mol^{-1} Å^{-2}). A conformational entropy energy term for side chains that was proportional to $N_{free} \ln 3$, in which N_{free} is the number of free variables, was also added.[32] The Monte Carlo based flexible docking algorithm is based on a global energy optimization method consisting of: 1) random conformational modification of a free variable according to a predefined continuous probability function, 2) local energy minization of differentiable variables,[33a] 3) total energy calculation including nondifferentiable energy terms such as entropy and solvation, and 4) acceptance or rejection according to the Metropolis criterion.[33b]

Ligand and protein docking: The first step was the full flexible docking into the PLA_2 pocket of a simple model consisting of a PM–lysine imine (PM-K). Ten independent global energy stochastic optimization simulations were run and the collected low-energy conformations were merged in a conformational ensemble.[34] Redundant poses of PM-K within 4 Å RMSD and those in which the lysine side chain of PM-K pointed inwards were eliminated (because these cannot form the PM–PLA_2 complex due to steric clashes); this left just two possible conformations of PM–K within the PLA_2 pocket. In each of these conformations, either the carboxylate or the aldehyde oxygen atom of PM makes a contact with the Ca^{2+} ion, in agreement with the experimental data on other ligands binding to PLA_2. No distance restraint was introduced between the Ca^{2+} atom and any of those oxygen atoms during the docking. The simulation temperature was set to $T = 1000$ K to improve conformational sampling. The PLA_2–PM–PLA_2 complex was then prepared by attaching a PM molecule to Lys67, in a similar way to that seen in the PM-K docking stage. This PLA_2–PM complex was considered as the "ligand" (in the sense that its six positional coordinates were considered to be free), and another PLA_2 molecule was regarded as the "receptor" (whose six positional coordinates were fixed). An initial ensemble of 128 protein–protein complexes was generated by randomizing the 6 torsion angles of the Lys67 chain attached to PM. Each complex within the ensemble was sub-

jected to a short local energy minimization by using a soft van der Waals interaction energy term.[35] The χ torsion angles of Lys67 and the six positional coordinates of the PLA_2–PM complex were set free during the minimization, whereas the tetracyclic carbon atoms of PM in PLA_2–PM were tethered to any of the ligand conformations found in the PM-K docking stage. Interface residues were identified for each of the 128 complexes, and a subsequent local energy minization step of each structure of the ensemble was undertaken. Side chains of all interface residues (collected from all structures of the ensemble), the six positional coordinates of the ligand, and the position of the Ca^{2+} atom were considered free during the energy minimization. A step procedure was used, in which the strength of the van der Waals interaction was gradually increased from zero to full interaction. A comparison of the Cα atoms of the ligand β sheet containing the PM+Lys67 (residues 67 to 79) was used to discard redundant complex structures. An RMSD threshold of 2.5 Å was used, which resulted in 17 diverse initial protein–protein complexes. Interface residues were reevaluated for the set of 17 complexes described above, and the list was expanded with those residues found within 4.0 Å of the interface residues. A stochastic global energy optimization was performed for each of the 17 complexes, with 2 independent runs per complex. The six positional coordinates of the ligand, the side chains at the interface, the torsional variables of PM+Lys67, and the Ca^{2+} atom were set free during the energy minimization. A total of 12 million energy evaluations was allowed, and low-energy conformations were stored in a conformational stack. Redundant conformations with respect to the Cα atoms of the ligand molecule were eliminated by using a low threshold of 0.7 Å, and the energy of the resulting ensemble (≈4400 structures) was further reevaluated by using an electrostatic energy term based on the solution of the Poisson equation with the boundary element algorithm. The set was further reduced by eliminating reduntant conformations within 1.0 Å RMSD. It is important to acknowledge that due to the inaccuracies in the force-field approximation and the lack of ad hoc parameter optimization, it is meaningless to consider only the best energy conformation as the most representative one. Instead, it is more meaningful to inspect the low-energy conformational states collected during the simulation. Remarkably, all but one within an energy window of 30 kcal mol^{-1} show the same conformational trend.

Molecular dynamics: Molecular dynamics (MD) simulations of the PLA_2–PM–PLA_2 complex were performed in a water box, which contains chlorine ions to neutralize any system charge. The box size was chosen to fit the molecular complex and to have at least 10 Å of water buffer on all sides of our solute. The CHARMM force field[36,37] was used. The solute complex has a nonstandard residue (PM) covalently bound to the ε-amino group of Lys67. The topology and parameters for the PM ligand were adopted from sterols.[38] Minimal adjustments were done by transferring and adjusting the standard bond, angle, and torsional parameters from standard lipids in the CHARMM force field. MD simulations were performed by using the NAMD 2.6 package.[39] First, the system was minimized by 1000 steps and annealed at 10 ps. The consequent system was MD simulated by using the Langevin barostat and thermostat[40] at ambient pressure and 300 K. A multistep scheme of nonbonded interactions was used with full electrostatic evaluations updated every four steps. The nonbonded-interaction cut off was set at 12 Å and the switching distance was 12 Å. Nonbonded electrostatic interactions were treated by using the Particle Mesh Ewald method.[41] The integration step was set to 1 fs, and energies and structures were stored after every 1 ps. The PLA_2–PM–PLA_2 complex was annealed at 1 ns and simulated for 10 ns.

Acknowledgements

We thank Prof. D. Wilton (University of Southampton) for kindly providing the N1A-PLA_2-IIA plasmid, S. Phatak (University of Texas at Houston) for helping with the manuscript, and C. Santomauro and the late Prof. A. Leone for their relevant contributions in the first steps of the project. Financial support by the University of Salerno and by MIUR (Rome) is gratefully acknowledged. The Italian authors also acknowledge the use of the instrumental facilities of the Centre of Competence in Diagnostics and Molecular Pharmaceutics supported by Regione Campania (Italy) through POR funds.

[1] O. G. Mouritsen in *Life—As a Matter of Fat: The Emerging Science of Lipidomics*, Springer, Berlin, **2005**.
[2] E. A. Dennis, *Adv. Exp. Med. Biol.* **1978**, *101*, 165–175.
[3] K. Best, A. Ohran, A. Hawes, T. Hazlett, E. Gratton, A. Judd, J. Bell, *Biochemistry* **2002**, *41*, 13982–13988.
[4] W. V. Winstead, J. Balsinde, E. A. Dennis, *Biochim. Biophys. Acta Mol.* **2000**, *1488*, 28–39.
[5] S. Bezzine, J. Bolling, A. G. Singer, S. L. Veateh, S. L. Keller, M. H. Gelb, *J. Biol. Chem.* **2002**, *277*, 48523–48534.
[6] S. Canaan, R. Nielsen, F. Ghomashchi, B. Robinson, M. Gelb, *J. Biol. Chem.* **2003**, *278*, 30984–30990.
[7] a) F. Dal Piaz, A. Casapullo, A. Randazzo, R. Riccio, P. Pucci, G. Marino, L. Gomez-Paloma, *ChemBioChem* **2002**, *3*, 664–671; b) M. C. Monti, A. Casapullo, R. Riccio, L. Gomez-Paloma, *Bioorg. Med. Chem.* **2004**, *12*, 1467–1474; c) M. C. Monti, A. Casapullo, R. Riccio, L. Gomez-Paloma, *FEBS Lett.* **2004**, *578*, 269–274; d) M. C. Monti, A. Casapullo, R. Riccio, L. Gomez-Paloma, *Rapid Commun. Mass Spectrom.* **2005**, *19*, 303–308; e) M. C. Monti, A. Casapullo, M. V. D'Auria, R. Riccio, L. Gomez-Paloma, *ChemBioChem* **2006**, *7*, 971–980; f) L. Gomez-Paloma, M. C. Monti, S. Terracciano, A. Casapullo, R. Riccio, *Curr. Org. Chem.* **2005**, *9*, 1419–1427; g) S. Terracciano, M. Rodriguez, M. Aquino, M. C. Monti, A. Casapullo, R. Riccio, L. Gomez-Paloma, *Curr. Med. Chem.* **2006**, *13*, 1947–1969.
[8] A. Randazzo, C. Debitus, L. Minale, P. Garcia Pastor, M. J. Alcazar, M. Payà, L. Gomez-Paloma, *J. Nat. Prod.* **1998**, *61*, 571–575.
[9] PM (**1**) has been the subject of a detailed in vitro and in vivo pharmacological investigation. It is able to reduce in a dose-dependent manner the levels of various proinflammatory mediators, such as prostaglandin E_2 (PGE_2), tumor necrosis factor α (TNFα), and leucotriene B_4 (LTB_4), and it has been shown to modulate the expression of inducible cyclooxygenase and nitric oxide synthetase (COX-2 and iNOS) by interfering with the nuclear factor κB (NF-κB) pathways. For further details, see: a) P. Garcia-Pastor, A. Randazzo, L. Gomez-Paloma, M. J. Alcaraz, M. Payà, *J. Pharmacol. Exp. Ther.* **1999**, *289*, 166–167; b) I. Posadas, M. C. Terencio, A. Randazzo, L. Gomez-Paloma, M. Payà, M. J. Alcaraz, *Biochem. Pharmacol.* **2003**, *65*, 887–895; c) J. Busserolles, M. Paya, M. V. D'Auria, L. Gomez-Paloma, M. J. Alcaraz, *Biochem. Pharmacol.* **2005**, *69*, 1433–1440.
[10] a) R. W. Schevitz, N. J. Bach, D. G. Carlson, N. Y. Chirgadze, D. K. Clawson, R. D. Dillaheim, S. E. Draheim, L. W. Hartley, N. D. Jones, E. D. Mihelich, J. L. Olkowski, D. W. Snyder, C. Sommers, J. P. Wery, *Nat. Struc. Biol.* **1995**, *2*, 458–465; b) J. Balsinde, M. Balboa, P. Insel, E. A. Dennis, *Annu. Rev. Pharmacol. Toxicol.* **1999**, *39*, 175–189; c) K. A. Hansford, R. C. Ried, C. I. Clark, J. D. Tyndall, M. W. Whitehouse, T. Guthrie, R. P. McGeary, K. Schafer, J. L. Martin, D. P. Fairlie, *ChemBiochem* **2003**, *4*, 181–185; d) M. D. Guerrero, M. Aquino, I. Bruno, M. C. Terencio, M. Paya, R. Riccio, L. Gomez-Paloma, *J. Med. Chem.* **2007**, *50*, 2176–2184.
[11] Q. Dong, M. Patel, K. F. Scott, G. G. Graham, P. J. Russell, P. Sved, *Cancer Lett.* **2006**, *240*, 9–16.
[12] a) G. V. Richieri, A. M. Klenfield, *Anal. Biochem.* **1995**, *229*, 256–263; b) T. Bayburt, M. Gelb, *Biochemistry* **1997**, *36*, 3216–3231.
[13] D. C. Wilton, *Biochem. J.* **1990**, *270*, 163–166.
[14] D. C. Wilton, *Biochem. J.* **1990**, *266*, 435–439.
[15] A. Shevchenko, M. Wilm, O. Worm, M. Mann, *Anal. Chem.* **1996**, *68*, 850–858.
[16] M. J. Cannon, G. A. Papalia, I. Navratilova, R. J. Fisher, L. R. Roberts, K. M. Worthy, A. G. Stephen, G. R. Marchesini, E. J. Collins, D. Casper, H. Qiu, D. Satpaev, S. F. Liparoto, D. A. Rice, I. I. Gorshkova, R. J. Darling, D. B. Bennett, M. Sekar, E. Hommema, A. M. Liang, E. S. Day, J. Inman, S. M. Karlicek, S. J. Ullrich, D. Hodges, T. Chu, E. Sullivan, J. Simpson, A. Rafique, B. Luginbühl, S. N. Westin, M. Bynum, P. Cachia, Y. J. Li, D. Kao, A. Neurauter, M. Wong, M. Swanson, D. G. Myszka, *Anal. Biochem.* **2004**, *330*, 98–113.

[17] C. N. Cavasotto, A. J. Orry, N. J. Murgolo, M. F. Czarnicki, S. A. Kocsi, B. E. Hawes, K. A. O'Neill, H. Hine, M. S. Burton, J. H. Voight, R. A. Abagyan, M. L. Bayne, F. J. Monsma, *J. Med. Chem.* **2008**, *51*, 581–588.
[18] C. N. Cavasotto, R. A. Abagyan, *J. Mol. Biol.* **2004**, *337*, 209–225.
[19] C. N. Cavasotto, G. Liu, S. Y. James, P. D. Hobbs, V. J. Peterson, A. A. Bhattacharya, S. K. Kolluri, X. K. Zhang, M. Leid, R. A. Abagyan, R. C. Liddington, M. I. Dawson, *J. Med. Chem.* **2004**, *47*, 4360–4372.
[20] C. N. Cavasotto, A. J. W. Orry, R. A. Abagyan, *Proteins Struct. Funct. Bioinf.* **2003**, *51*, 423–433.
[21] M. C. Monti, A. Casapullo, C. N. Cavasotto, A. Napolitano, R. Riccio, *ChemBioChem* **2007**, *8*, 1585–1591.
[22] The different chromatographic profile of PM when it is submitted in the presence or absence of DOPG micelles to low-resolution size-exclusion chromatography supported this hypothesis (data not shown). Actually, after preincubation with the micelles, PM was recovered coeluting with the DOPG vesicles in a unique chromatographic fraction.
[23] a) G. V. Richieri, A. M. Kleinfield, *Anal. Biochem.* **1995**, *229*, 256–263; b) A. Kinkaid, D. C. Wilton, *Biochem. J.* **1991**, *278*, 843–848.
[24] A. Buckland, D. C. Wilton, *Biochim. Biophys. Acta* **1998**, *1391*, 367–376.
[25] U. K. Laemmli, *Nature* **1970**, *227*, 680–685.
[26] A. Shevchenko, M. Wilm, O. Worm, M. Mann, *Anal. Chem.* **1996**, *68*, 850–858.
[27] R. Abagyan, M. Totrov, D. Kuznetsov, *J. Comput. Chem.* **1994**, *15*, 488–506.
[28] F. A. Momany, R. F. McGuire, A. W. Burgess, H. A. Scheraga, *J. Phys. Chem.* **1975**, *79*, 2361–2381.
[29] G. Nemethy, K. D. Gibson, K. A. Palmer, C. N. Yoon, M. G. Paterlini, A. Zagari, S. Rumsey, H. A. Scheraga, *J. Phys. Chem.* **1992**, *96*, 6472–6484.
[30] T. Ooi, M. Oobatake, G. Nemethy, H. A. Scheraga, *Proc. Natl. Acad. Sci. USA* **1987**, *84*, 3086–3090.
[31] M. Totrov, R. Abagyan, *Biopolymers* **2001**, *60*, 124–133.
[32] R. Abagyan, M. Totrov, *J. Mol. Biol.* **1994**, *235*, 983–1002.
[33] a) Z. Li, H. A. Scheraga, *Proc. Natl. Acad. Sci. USA* **1987**, *84*, 6611–6615; b) N. A. Metropolis, A. W. Rosenbluth, N. M. Rosenbluth, A. H. Teller, E. Teller, *J. Chem. Phys.* **1953**, *21*, 1087–1092.
[34] R. Abagyan, P. Argos, *J. Mol. Biol.* **1992**, *225*, 519–532.
[35] M. Totrov, R. Abagyan in *Drug–receptor thermodynamics: Introduction and experimental applications* (Ed.: R. B. Raffa), Wiley, New York, **2001**.
[36] A. D. MacKerell, D. Bashford, M. Bellott, R. L. Dunbrack, J. D. Evanseck, M. J. Field, S. Fischer, J. Gao, H. Guo, S. Ha, D. Joseph-McCarthy, L. Kuchnir, K. Kuczera, F. T. K. Lau, C. Mattos, S. Michnick, T. Ngo, D. T. Nguyen, B. Prodhom, W. E. Reiher, B. Roux, M. Schlenkrich, J. C. Smith, R. Stote, J. Straub, M. Watanabe, J. Wiorkiewicz-Kuczera, D. Yin, M. Karplus, *J. Phys. Chem. B* **1998**, *102*, 3586–3616.
[37] M. Schlenkrich, J. Brickmann, A. D. MacKerell, M. Karplus, *Biological Membranes: A Molecular Perspective from Computation and Experiment* (Eds.: K. M. Merz, B. Roux), Birkhauser, Boston, **1996**, p. 31.
[38] Z. Cournia, J. C. Smith, G. M. Ullmann, *J. Comput. Chem.* **2005**, *26*, 1383–1399.
[39] J. C. Phillips, R. Braun, W. Wang, J. Gumbart, E. Tajkhorshid, E. Villa, C. Chipot, R. D. Skeel, L. Kale, K. Schulten, *J. Comput. Chem.* **2005**, *26*, 1781–1802.
[40] S. Feller, Y. H. Zhang, R. W. Pastor, B. R. Brooks, *J. Chem. Phys.* **1995**, *103*, 4613–4621.
[41] T. Darden, D. York, L. Pedersen, *J. Chem. Phys.* **1993**, *98*, 10089–10092.

Received: July 24, 2008
Revised: October 15, 2008
Published online: December 9, 2008

